

Spatial Control of 3D Energy Transfer in Supramolecular Nanostructured Host–Guest Architectures

Lucas Viani,[†] Lars Poulsen Tolbod,^{‡,§} Mikael Jazdyk,^{||} Greta Patrinoiu,^{⊥,#} Fabrizio Cordella,[∇] Andrea Mura,[∇] Giovanni Bongiovanni,[∇] Chiara Botta,[⊥] David Beljonne,[†] Jérôme Cornil,[†] Michael Hanack,^{||} Hans-Joachim Egelhaaf,^{‡,○} and Johannes Gierschner^{*,†,◆}

Laboratory for Chemistry of Novel Materials, University of Mons-Hainaut, Place du Parc 20, B-7000 Mons, Belgium, Institute of Physical and Theoretical Chemistry, University of Tübingen, Auf der Morgenstelle 8, D-72076 Tübingen, Germany, Department of Nuclear Medicine, Aarhus University Hospital, Noerrebrogade 44, 8000 Aarhus C, Denmark, Institute of Organic Chemistry, University of Tübingen, Auf der Morgenstelle 18, D-72076 Tübingen, Germany, Istituto per lo Studio delle Macromolecole, C.N.R., via Bassini 15, 20133, Milan, Italy, Ilie Murgulescu Institute of Physical Chemistry, Independentei 202, 060021 Bucharest, Romania, Dipartimento di Fisica and Istituto Nazionale di Fisica della Materia, Università degli Studi di Cagliari, I-09042 Monserrato (CA), Italy, Christian-Doppler Laboratory for Surface Optical Methods, Institute for Semiconductor Physics, Johannes-Kepler-University, Altenbergerstr. 69, A-4040 Linz, Austria, Present address: Konarka Technologies GmbH, Landgrabenstrasse 94, D-90443 Nürnberg, and Madrid Institute for Advanced Studies, IMDEA Nanoscience, Modulo, C-IX, Av. Tomás y Valiente 7, Campus de Cantoblanco, 28049 Madrid, Spain

Received: May 12, 2009; Revised Manuscript Received: June 29, 2009

Systematic control of 3D energy transfer (ET) dynamics is achieved in supramolecular nanostructured host–guest systems using spacer-functionalized guest chromophores. Quantum chemistry-based Monte Carlo simulations reveal the strong impact of the spacer length on the ET dynamics, efficiency, and dimensionality. Remarkably high exciton diffusion lengths demonstrate that there is ample scope for optimizing oligomeric or polymeric optoelectronic devices.

Resonant energy transfer (ET) is a fundamental process in light harvesting by biological systems that can also be exploited for funneling electronic excitations in optoelectronic devices. The increasing interest in tailor-made organic conjugated materials for these devices requires a thorough understanding of diffusion-enhanced three-dimensional (3D) ET and modeling of intermolecular interactions beyond the classical Förster picture due to the close proximity of the molecules in solid-state device architectures.¹ New preparative approaches, such as supramolecular donor–acceptor systems,^{2,3} in hand with a realistic theoretical description might tap the full potential of material design for optimized devices.

In recent years, increasing attention has been paid to highly ordered supramolecular nanostructured host–guest compounds (HGCs), based either on organic^{4–14} or on inorganic *optically inert* hosts;^{15–17} in such systems, the degree of both energetic and positional disorder is small, leading to enhanced properties for optoelectronic applications.^{9–12,15} In a previous study, we

have used the organic nanochannel forming host perhydrotriphenylene (PHTP) to investigate 3D ET processes between weakly coupled chromophores by including rod-like donor (D) and acceptor (A) molecules at low A:D ratios.⁹ By running Monte Carlo (MC) simulations and treating ET on a quantum-chemical level, we were able to describe 3D ET in these systems quantitatively without using adjustable parameters. In the present study, we go a step further by using donor molecules with terminal alkyl spacer groups to systematically vary the distance between the centers of two adjacent donor moieties from 2 to 6 nm, thus gaining full spatial control of 3D ET. By combining experiments and simulations, we are able to understand the details of electronic excitation dynamics, in particular the length and directionality of exciton diffusion, as a function of intermolecular separation. In this respect, our MC approach provides a flexible toolbox for future design of optimized materials for optoelectronic applications.

The systems under study are presented in Figure 1. The donor molecules *n*SDSB are derived from *p,p*-distyrylbenzene (DSB) by attaching two terminal H(CH₂)_{*n*}O– substituents of variable lengths (with *n* the number of carbon atoms). The acceptor molecule quinquethiophene (5T) is added at molar doping ratios (*x*_{5T}) ranging from 10^{–4} to 10^{–1}. The guest molecules are embedded in the channels of the pseudo-hexagonal PHTP host lattice, adjacent molecules in the same channel being in van der Waals contact, as supported by comparison of force-field calculations with quantitative UV/vis and ¹H NMR data.² The separation between the channels is about 1.5 nm, which

* Corresponding author. E-mail: johannes.gierschner@imdea.org.

† University of Mons-Hainaut.

‡ Institute of Physical and Theoretical Chemistry, University of Tübingen.

§ Aarhus University Hospital.

|| Institute of Organic Chemistry, University of Tübingen.

⊥ Istituto per lo Studio delle Macromolecole.

Ilie Murgulescu Institute of Physical Chemistry.

∇ Università degli Studi di Cagliari.

○ Johannes-Kepler-University.

◆ IMDEA Nanoscience.

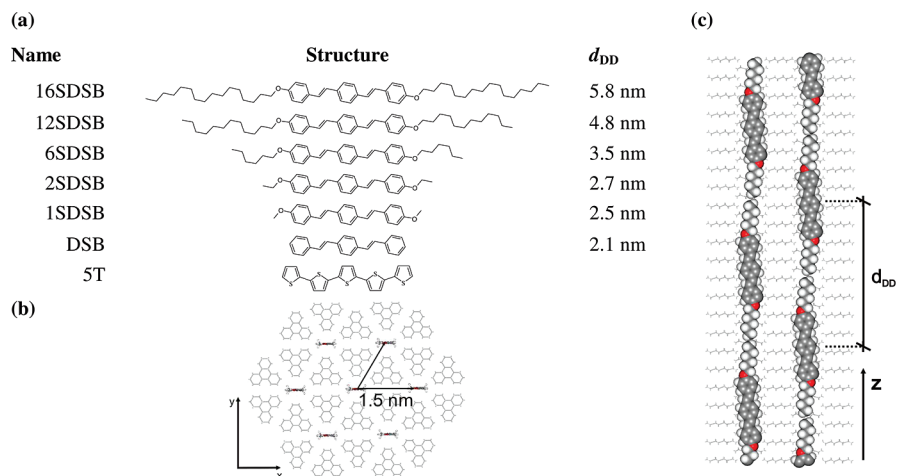


Figure 1. Chemical structures of the investigated systems. (a) Donor (n SDSB) and acceptor (5T) guest molecules, with d_{DD} (in nm) indicating the intrachannel donor–donor distances. (b) Top view of the HGC in the direction of the channel axis (z). (c) Side view. For details, see ref 2.

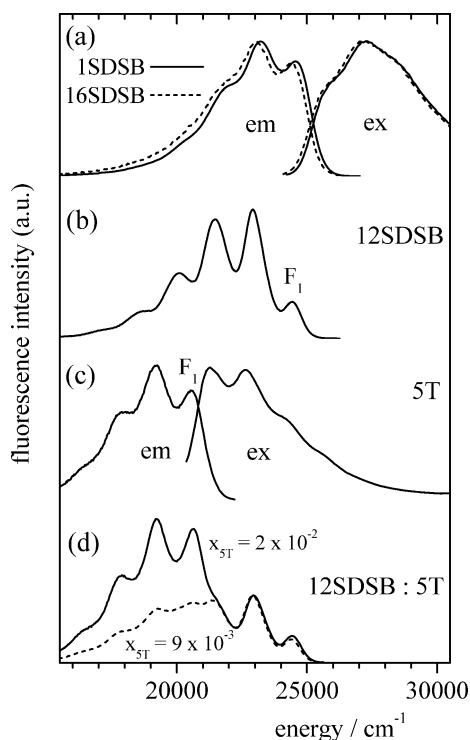


Figure 2. Fluorescence emission (em) and excitation (ex) spectra of the oligomers: (a) 1SDSB and 16SDSB in solution (benzene); (b) 12SDSB in PHTP; (c) 5T in PHTP and (d) 12SDSB:5T in PHTP (at two different doping ratios x_{5T}). Spectra are normalized to the maximum of the donor emission.

efficiently suppresses side-by-side interactions between the guests.² In solution, the emission and absorption spectra of n SDSB are independent of spacer length n , since the end groups hardly perturb the electronic structure of the chromophore; see Figure 2. The spectra in the HGCs are slightly red-shifted against solution,² while the first fluorescence band (F_1) is typically somewhat suppressed by self-absorption in the solid-state samples. The fluorescence quantum yields ($\Phi_F = 0.9$ –1.0, from absolute measurements) and decay times ($\tau_F = 1.0$ –1.6 ns, depending somewhat on the sample) of n SDSB in PHTP are close to the solution values ($\Phi_F = 0.9$, $\tau_F = 1.0$ –1.2 ns), thus demonstrating that the bright fluorescent properties in solution are preserved in the solid state.

The emission of n SDSB overlaps well with the absorption of 5T (Figure 2), a condition required for efficient ET.

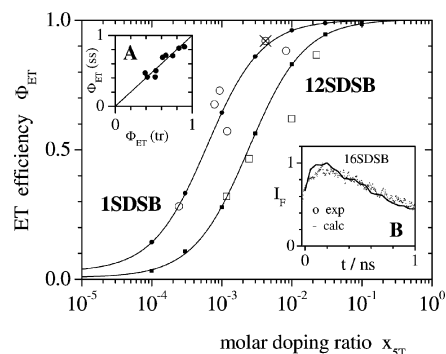


Figure 3. Experimental (open symbols) and calculated (closed symbols) steady-state ET efficiency Φ_{ET} as a function of x_{5T} for 1SDSB (circles) and 12SDSB (squares). Lines are guides to the eye. The cross indicates an experimental value from absolute measurements. Inset A: correlation diagram of Φ_{ET} determined from steady-state (ss) vs time-resolved (tr) measurements. Inset B: experimental (dots) and calculated (line) donor time trace of 16SDSB at $x_{5T} = 7 \times 10^{-2}$.

Experimental ET efficiencies Φ_{ET} as determined via eq 1 from steady-state spectra for donors with two different spacer lengths, 1SDSB and 12SDSB, as a function of the doping ratio x_{5T} are shown in Figure 3, together with a typical donor emission decay curve. Φ_{ET} values calculated from steady-state emission intensities (measured both with and without integrating sphere) compare well to those deduced from the reduction of the donor decay times upon doping via eq 2; see the inset of Figure 3. The values of Φ_{ET} increase significantly both with increasing doping ratio x_{5T} and with decreasing spacer length n ; see Figure 3.

For the corresponding theoretical description of the ET process, the HGC structure is represented by an ideal hexagonal network of parallel channels with an interchannel separation of 1.5 nm and intrachannel distances between the centers of the guests dictated by their van der Waals lengths; see Figure 1. The acceptors (5T) are randomly distributed within the lattice. The MC simulation follows the scheme described in ref 9, using electronic couplings calculated quantum-chemically according to the distributed monopole approach (DMA, see eq 4). The empirical parameters entering the simulations are the DD and DA spectral overlaps ($J_{DD} = 8.8 \times 10^{-6}$ cm, $J_{DA} = 1.52 \times 10^{-4}$ cm) as well as the fluorescence lifetimes ($\tau_D = 1.6$ ns, $\tau_A = 0.9$ ns). No adjustable parameters are used. The simulations were performed on large systems with approximately 10^6

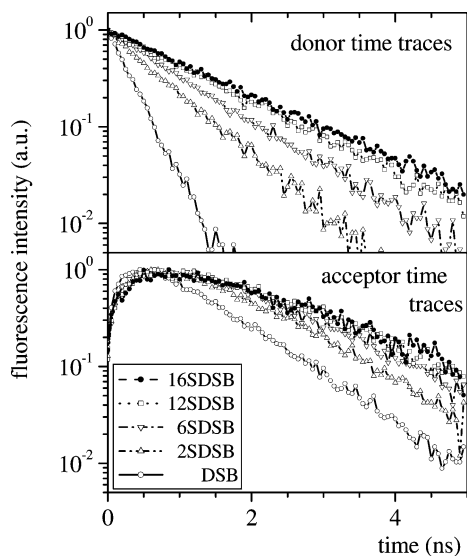


Figure 4. Calculated time-resolved fluorescence of donor (top) and acceptor (bottom) molecules ($x_{5T} = 1.0 \times 10^{-3}$) for different spacer lengths n SDSB.

molecules (thus close to the actual size of HGCs) to minimize the effects of the periodic boundary conditions which were applied.

The simulated transfer efficiencies, Φ_{ET} , and excited-state dynamics for n SDSB agree quite well with the experimental results; see Figure 3. However, the real merit of the simulations lies in the elucidation of the excited-state dynamics in time and space at the microscopic scale. This is demonstrated by the impact of the alkyl spacer length n and hence of the intrachannel distances on the donor and acceptor fluorescence time traces; see Figure 4. A decrease in the intermolecular separation along the channels leads to a substantial reduction of τ_D and to a shorter risetime for the acceptor emission. This results in a significant enhancement of Φ_{ET} , e.g., by more than 40% at $x_{5T} = 10^{-3}$ upon reducing the spacer length from $n = 12$ to $n = 1$; see Figure 3. Moreover, the simulations show that the variation of the spacer length changes the directionality of energy migration throughout the crystal. Figure 5a depicts the spatial distribution of exciton decay probability for different spacer lengths for a structure with uncorrelated interchannel positions of the guest molecules; the corresponding number of intra- and interchannel transfer steps is given in Figure 5b. With increasing n , the ET mechanism switches from quasi 1D for DSB, where it has a strong intrachannel character, to quasi 3D for $n = 1$

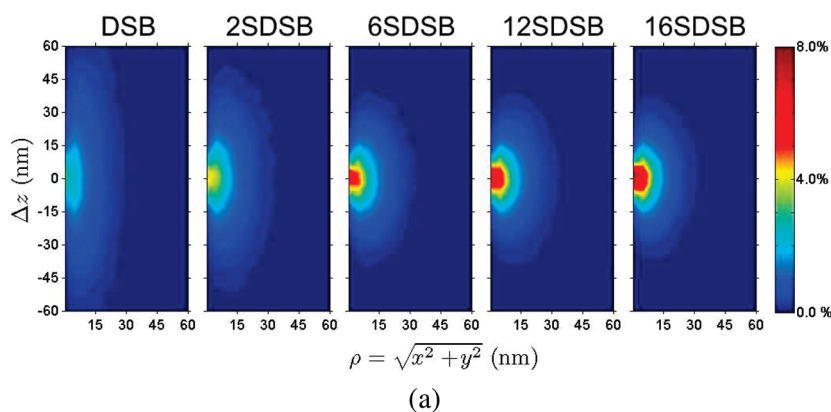


Figure 5. Calculated excited-state dynamics for n SDSB at $x_{5T} = 1.2 \times 10^{-3}$. Left: distance covered from the initial site of excitation to the site of decay. Right: calculated average number of transfer steps as a function of the D–D separation.

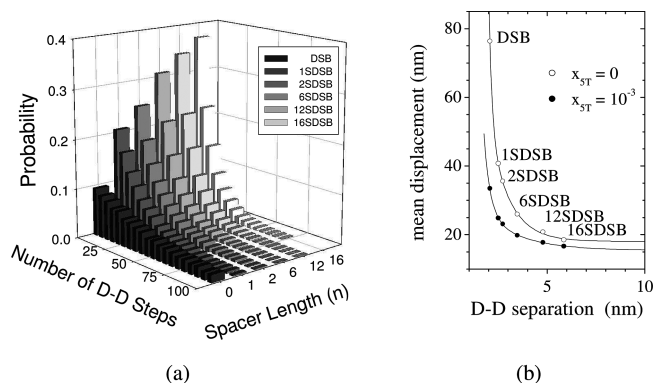


Figure 6. Calculated excited-state dynamics for n SDSB. Left: histogram of the number of D–D steps during the diffusion process for the different spacer lengths n ($x_{5T} = 1.2 \times 10^{-3}$). Right: diffusion length (MSD) as a function of the D–D separation at $x_{5T} = 10^{-3}$ and $x_{5T} = 0$.

and a quasi 2D interchannel transport for $n > 6$. For a hypothetical structure with correlated guest positions (i.e., a layered crystal structure), the energy migration becomes purely 2D for large n . This trend can be rationalized by the dramatic reduction of the excitonic coupling V_{DX} between nearest neighbors inside the channel with increasing n . The lower probability of intrachannel transfers (which are responsible for the long migration path in the DSB:5T case) strongly reduces the number of donor–donor (D–D) hopping steps (Figure 6a); in turn, this leads to a decrease in the diffusion length (related to the exciton mean square displacement¹⁸ which drops from 33 nm for DSB to 17 nm for 16SDSB at a doping ratio of $x_{5T} = 10^{-3}$; see Figure 6b. Consequently, while the doping ratio x_{5T} strongly affects the diffusion length for small D–D separations (compare, e.g., the trap free case, $x_{5T} = 0$, with $x_{5T} = 10^{-3}$ for DSB in Figure 6b), it plays only a minor role for large D–D separations (as in the latter case, the electronic excitations decay before having reached an acceptor).

In conclusion, we have prepared supramolecular nanostructured host–guest systems, where the spacer functionalization of the guests is used to systematically control efficiency and dimensionality of ET between the weakly coupled chromophores. All experimental results are fully reproduced by MC simulations based on a quantum-chemical description of the transfer rates which yield a spatial and temporal description of the excited-state dynamics without using adjustable parameters. Despite the rather large intermolecular separations in the supramolecular architecture, the remarkably high diffusion

length of the electronic excitations, which is comparable to, e.g., polycrystalline pentacene,¹⁹ demonstrates that there is ample scope for the optimization of exciton diffusion in densely packed oligomeric or polymeric samples via the proper design of exciton coupling (essentially through optimized conjugation length and packing),²⁰ spectral overlap, and excited-state lifetimes.

Experimental and Computational Details

Synthesis. For the synthesis of the oligomers *n*SDSB, the respective 4-alkoxybenzaldehyde (RO-BZA) derivatives were prepared in a Williamson synthesis from 4-hydroxy-BZA and 1-bromoalkane in a potassium carbonate/acetonitrile solution.²¹ The RO-BZAs were then reacted in a Wittig reaction with *p*-xylylenebis(triphenylphosphonium bromide)²² to yield *n*SDSB. PHTP was provided by Dr. Borchers (BASF, Ludwigshafen, Germany).

Sample Preparation. Solutions of the compounds were prepared in benzene (spectroscopic grade) with absorbance <0.1. PHTP/*n*SDSB/5T HGCs were prepared by transferring a small amount of 5T benzene solution to an ampule and removing the solvent under vacuum. Subsequently, solid PHTP and *n*SDSB were added using a large excess of PHTP relative to the ideal PHTP/*n*SDSB molar ratio of 9:1. The ampules were sealed under vacuum and heated to 260 °C. The resulting crystalline powders were smeared onto quartz plates to yield layers of a few micrometers used for the spectroscopic investigations.

Spectroscopy. Steady-state fluorescence spectra were recorded at right angle on a SPEX 222 fluorometer equipped with two 0.25 m double monochromators, a 150 W vertical xenon arc lamp (Müller Electronics) and a photomultiplier tube (Hamamatsu R928). All emission and excitation spectra were corrected for the characteristics of the detection system and lamp source, respectively. Time-resolved emission spectra were measured using a ps-setup consisting of a frequency-doubled Ti:sapphire laser (Spectra Physics, Tsunami, $\lambda = 390$ nm, repetition rate 80 MHz), 410 nm cutoff filter, and a streak camera (Hamamatsu C5680) coupled to an imaging monochromator. To avoid bimolecular processes and sample degradation, the mean laser power was kept below 1 μ W. Absolute fluorescence quantum yields were determined with an integrating sphere.⁸

Data Evaluation. The ET efficiency, Φ_{ET} , is defined as the fraction of photons absorbed by D and transferred to A. In steady-state conditions, Φ_{ET} is determined from the ratio between the integrated fluorescence intensities of the donor, I_{D} , and of the acceptor, I_{A} , upon selective excitation of D

$$\Phi_{\text{ET}} = \left(1 + \frac{\Phi_{\text{A}}}{\Phi_{\text{D}}} \cdot \frac{I_{\text{D}}}{I_{\text{A}}}\right)^{-1} \quad (1)$$

where Φ_{D} and Φ_{A} are the fluorescence quantum yields of pure D and A samples in PHTP. The condition of selective excitation of D is fulfilled in our system due to the very low A concentration, which makes direct excitation of A negligible. In time-resolved experiments, Φ_{ET} can be determined from the reduction of the (exponential) lifetime of D due to ET, where $\tau_{\text{D/A}}$ and τ_{D} are the lifetimes of D in the presence and absence of A, respectively.

$$\Phi_{\text{ET}} = 1 - \tau_{\text{D/A}}/\tau_{\text{D}} \quad (2)$$

Calculation of Energy Transfer. The description of exciton migration is derived via Fermi's golden rule as

$$k_{\text{ET}}(\text{DX}) = \frac{2\pi}{\hbar} |V_{\text{DX}}|^2 \cdot s^2 J_{\text{DX}} \quad (3)$$

where V_{DX} is the exciton coupling between the initial (D*X) and the final state (DX*), with "X" being D or A, s^2 is the screening factor, and J_{DX} is the spectral overlap between the emission spectrum of D and the absorption spectrum of "X", both area-normalized on the energy scale. As shown in a previous work,⁹ the classical Förster point-dipole approach (PDA) can be used to describe the exciton couplings in HGCs only for low dye concentration, i.e., large intermolecular separations. Otherwise, the PDA underestimates intrachannel and overestimates interchannel transfers, respectively. Since directionality of exciton migration is a key issue of this work, we have adopted the more general distributed monopole approach to calculate all excitonic interactions, which gives

$$V_{\text{DX}} = \frac{1}{4\pi\epsilon_0} \sum_i \sum_j \frac{q_{\text{D}}(i) q_{\text{X}}(j)}{R_{\text{DX}}(i,j)} \quad (4)$$

where $q_{\text{D}}(i)$ and $q_{\text{X}}(j)$ are the atomic transition densities (ATD) over atoms i and j belonging to molecules D and X, respectively; $R_{\text{DX}}(i,j)$ is the distance between the atoms. The screening factor s was considered to be $1/n^2$, i.e., like in the Förster expression, which is reasonable since the coupling of the dyes is in the weak regime. ATD values were determined from ZINDO/S calculations (Zerner's spectroscopic parametrization for the semiempirical Hartree–Fock intermediate neglect of differential overlap)²³ on the basis of geometries optimized at the semiempirical Hartree–Fock AM1 (Austin Model 1) level,²⁴ imposing planar conformations for the conjugated backbone. Cutoff distances for the exciton couplings were used, ranging from 4 nm for DSB up to 13 nm for 16SDSB.

Acknowledgment. This work was supported by the European Commission (EC) through the Human Potential Program (Marie-Curie Research Training Networks NANOCHANNEL Contract No. HPRN-CT-2002-00323, and NANOMATCH, MRTN-CT-2006-035884) and by the EC STREP project MODECOM (NMP-CT-2006-016434). D.B. and J.C. are Research Associates of the FNRS. J.G. is a "Ramón y Cajal" research fellow, financed by the Spanish Ministry for Science and Innovation.

References and Notes

- (1) For recent reviews see: (a) Scholes, G. D. *Annu. Rev. Phys. Chem.* **2003**, *54*, 57. (b) Hsu, C.-P. *Acc. Chem. Res.* **2009**, *42*, 509. (c) Saini, S.; Srinivas, G.; Bagchi, B. *J. Phys. Chem. B* **2009**, *113*, 1817. (d) Beljonne, D.; Curutchet, C.; Scholes, G. D.; Silbey, R. J. *J. Phys. Chem. B* **2009**, *113*, 6583.
- (2) (a) Ajayaghosh, A.; George, S. J.; Praveen, V. K. *Angew. Chem., Int. Ed.* **2003**, *42*, 332. (b) Hoeben, F. J. M.; Jonkheijm, P.; Meijer, E. W.; Schenning, A. P. H. J. *Chem. Rev.* **2005**, *105*, 1491. (c) Guerso, A. D.; Olive, A. G. L.; Reichwagen, J.; Hopf, H.; Desvergne, J.-P. *J. Am. Chem. Soc.* **2005**, *127*, 17984.
- (3) (a) Oelkrug, D.; Tompert, A.; Gierschner, J.; Egelhaaf, H.-J.; Hanack, M.; Hohloch, M.; Steinhuber, E. *J. Phys. Chem. B* **1998**, *102*, 1902. (b) Egelhaaf, H.-J.; Gierschner, J.; Oelkrug, D. *Synth. Met.* **2002**, *127*, 221.
- (4) (a) Gierschner, J.; Luer, L.; Oelkrug, D.; Musluoglu, E.; Behnisch, B.; Hanack, M. *Adv. Mater.* **2000**, *12*, 757. (b) Gierschner, J.; Egelhaaf, H.-J.; Mack, H.-G.; Oelkrug, D.; Martinez Alvarez, R.; Hanack, M. *Synth. Met.* **2003**, *137*, 1449.
- (5) Brustolon, M.; Barbon, A.; Bortolus, M.; Maniero, A. L.; Sozzani, P.; Comotti, A.; Simonutti, R. *J. Am. Chem. Soc.* **2004**, *126*, 15512.
- (6) Wilson, J. S.; Frampton, M. J.; Michels, J. J.; Sardone, L.; Marletta, G.; Friend, R. H.; Samorí, P.; Anderson, H. L.; Cacialli, F. *Adv. Mater.* **2005**, *17*, 2659.
- (7) Kim, O.-K.; Je, J.; Melinger, J. S. *J. Am. Chem. Soc.* **2006**, *128*, 4532.

(8) Moreau, J.; Giovanella, U.; Bombenger, J.-P.; Porzio, W.; Vohra, V.; Spadacini, L.; Di Silvestro, G.; Barba, L.; Arrighetti, G.; Destri, S.; Pasini, M.; Saba, M.; Quochi, F.; Mura, A.; Bongiovanni, G.; Fiorini, M.; Uslenghi, M.; Botta, C. *ChemPhysChem* **2009**, *10*, 647–653.

(9) Poulsen, L.; Jazdzzyk, M.; Communal, J.-E.; Sancho-García, J. C.; Mura, A.; Bongiovanni, G.; Beljonne, D.; Cornil, J.; Hanack, M.; Egelhaaf, H.-J.; Gierschner, J. *J. Am. Chem. Soc.* **2007**, *129*, 8585.

(10) (a) Botta, C.; Patrinoiu, G.; Picouet, P.; Yunus, S.; Communal, J.-E.; Cordella, F.; Quochi, F.; Mura, A.; Bongiovanni, G.; Pasini, M.; Destri, S.; Di Silvestro, G. *Adv. Mater.* **2004**, *16*, 1716. (b) Bongiovanni, G.; Botta, C.; Brédas, J. L.; Cornil, J.; Ferro, D. R.; Mura, A.; Piaggi, A.; Tubino, R. *Chem. Phys. Lett.* **1997**, *278*, 146.

(11) Komorowska, K.; Brasselet, S.; Dutier, G.; Ledoux, I.; Zyss, J.; Poulsen, L.; Jazdzzyk, M.; Egelhaaf, H.-J.; Gierschner, J.; Hanack, M. *Chem. Phys.* **2005**, *318*, 12.

(12) Langley, P. J.; Hulliger, J. *Chem. Soc. Rev.* **1999**, *28*, 279.

(13) Vásquez, S. O. *Phys. Chem. Chem. Phys.* **2008**, *10*, 5459.

(14) Srinivasan, G.; Villanueva-Garibay, J. A.; Müller, K.; Oelkrug, D.; Milián Medina, B.; Beljonne, D.; Cornil, J.; Wykes, M.; Viani, L.; Gierschner, J.; Martínez Alvarez, R.; Jazdzzyk, M.; Hanack, M.; Egelhaaf, H.-J. *Phys. Chem. Chem. Phys.* **2009**, *11*, 4996.

(15) Calzaferrri, G.; Huber, S.; Maas, H.; Minkowski, C. *Angew. Chem., Int. Ed.* **2003**, *42*, 3732.

(16) Nguyen, T.-Q.; Wu, J.; Doan, V.; Schwartz, B. J.; Tolbert, S. *Science* **2000**, *288*, 652.

(17) Shekhar, S.; Aharon, E.; Tian, N.; Galbrecht, F.; Scherf, U.; Holder, E.; Frey, G. L. *ChemPhysChem* **2009**, *10*, 576.

(18) The MSD can be correlated to the diffusion length as $d_L = (6D\tau_{\text{DA}})^{1/2} = \langle |r_i(t_i) - r_i(0)|^2 \rangle^{1/2}$ with D the diffusion coefficient, τ_{DA} the fluorescence lifetime of D in the presence of A, and $r_i(0)$ and $r_i(t_i)$ the initial and final positions of the excitation. This relation holds true only if the displacement is linear in time, which is not always the case in the simulations; thus, we choose to report MSD rather than d_L .

(19) Peumans, P.; Yakimov, A.; Forrest, S. R. *J. Appl. Phys.* **2003**, *93*, 3693.

(20) Gierschner, J.; Huang, Y.-S.; Van Averbeke, B.; Cornil, J.; Friend, R. H.; Beljonne, D. *J. Chem. Phys.* **2009**, *130*, 044105.

(21) Ndayikengurukiye, H.; Jacobs, S.; Tachelet, W.; Van Der Looy, J.; Pollaris, A.; Geise, H. J.; Claeys, M.; Kauffmann, J. M.; Janietz, S. *Tetrahedron* **1997**, *53*, 13811.

(22) Sancho Garcia, J. C.; Brédas, J. L.; Beljonne, D.; Cornil, J.; Martínez Alvarez, R.; Hanack, M.; Poulsen, L.; Gierschner, J.; Mack, H.-G.; Egelhaaf, H.-J.; Oelkrug, D. *J. Phys. Chem. B* **2005**, *109*, 4872.

(23) Zerner, M. C. In *Reviews in Computational Chemistry*; Boyd, D. B., Ed.; Wiley VCH: New York, 1994; Vol. II, p 313.

(24) Dewar, M. J. S.; Zoebish, E. G.; Healy, E. F.; Stewart, J. J. P. *J. Am. Chem. Soc.* **1985**, *107*, 3902.

JP904415Z